Chapter 4

Harmonic Minimization in HC-MLI Using Modified Grey Wolf Optimization

4.1 Introduction

In this chapter, selective harmonics elimination pulse width modulation (SHE-PWM) technique has been employed through modified grey wolf optimisation (MGWO). This optimization algorithm is then applied for the control of a three-phase, 11-level hybrid cascaded multilevel inverter (HC-MLI) [114]. SHE-PWM technique is implemented through MGWO which generates optimal switching angles for the HC-MLI, so as to eliminate lower order harmonics such as 5^{th}, 7^{th}, 11^{th} and 13^{th} from the output voltage. The capacitor voltage balance is achieved even at higher modulation indices by exploiting the redundant switching states of HC-MLI.

4.2 Mathematical Modelling of GWO Algorithm

GWO algorithm mimics the hunting mechanism and leadership hierarchy of grey wolves. GWO uses four main steps to achieve the best positions such as searching, encircling, hunting and attacking the prey [97], [98]. The algorithm consists of four types of grey wolves which are alpha (α), beta (β), delta (δ) and omega (ω). In this section, the mathematical models of the social hierarchy, encircling, search of prey, attacking prey and hunting mechanism are discussed. In order to mathematically model the social hierarchy of wolves, α is considered as the fittest solution. Consequently, the second and third best solutions are named β and δ respectively. The rest of the candidate solutions are assumed to be omega ω. In the GWO algorithm the hunting (optimization) is guided by α, β and δ.

4.2.1 Encircling Prey

The grey wolves update their positions around the prey using (4.1) and (4.2), given as

$$D = \left|\vec{C} \cdot \vec{X}_P(j) - \vec{X}(j)\right| \tag{4.1}$$

$$\vec{X}(j+1) = \vec{X}_P(j) - \vec{A}.\vec{D} \tag{4.2}$$

where j is the current iteration. X indicates the position vector of the grey wolf. X_p is the position vector of the prey. A and C are coefficient vectors. Vector A is expressed as

$$\vec{A} = 2\vec{a}.\vec{r}_1 - \vec{a} \tag{4.3}$$

and vector C as

$$\vec{C} = 2.\vec{r}_2 \tag{4.4}$$

where a is a coefficient vector. r_1 and r_2 are random vectors. The value of a linearly decreases from [2, 0] and r_1, r_2 are random vectors between [0, 1].

A two-dimensional position vector and some of the possible update co-ordinates are demonstrated in Fig. 4.1. The grey wolf in position (X, Y) can update its position according to the position of the prey (X^*, Y^*) as shown in Fig. 4.1. Different places around the best agent can be reached with respect to the current position by adjusting the value of A and C vectors.

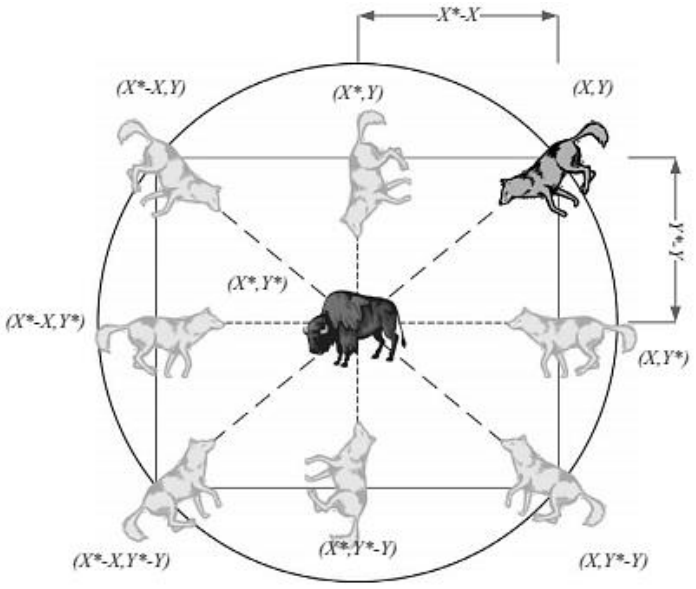

Fig. 4.1 2D vectors and their possible next locations in GWO [97].

4.2.2 Attacking Prey (Exploitation Phase)

In order to mathematically model the attacking the prey, the value of $\vec{a}$ decreased in due course iterations. The value of a linearly decreases from [2, 0] and r_1, r_2 are random vectors between [0, 1]. The value of a is within the range [1, 2] at early stage. A becomes greater than 1 or less than −1 in due course of time. This helps the grey wolves to diverge from the currently considered prey to find a better prey. When, a decreases and comes within the range [0,1], A lies in the range [−1, 1], which compels the grey wolves to move gradually towards the best position. With these operators, the GWO algorithm allows its search agents to update their position based on the location of the α, β and δ and attack towards the prey. However, the GWO algorithm is prone to stagnation in local solutions with these operators.

4.2.3 Search for Prey (Exploration Phase)

Grey wolves mostly search according to the position of the α, β and δ wolves. They diverge from each other to search for prey and converge to attack prey. In order to mathematically model exploration, the value of $\vec{A}$ is set at a value greater than 1 or less than -1. This emphasizes exploration and allows the GWO algorithm to search globally. Fig. 4.2(a) shows that $|\vec{A}| < 1$ forces the wolves to attack the prey and Fig. 4.2(b) shows that $|\vec{A}| > 1$ forces the grey wolves to diverge from the prey.

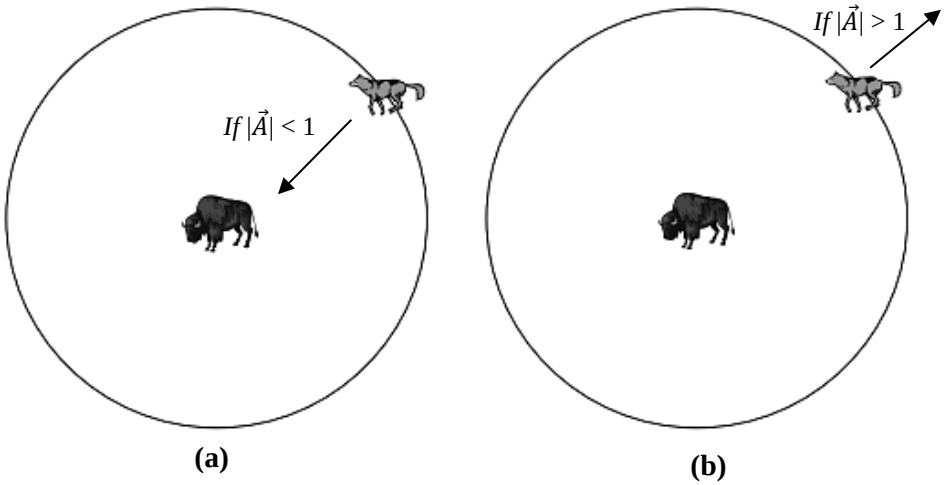

Fig. 4.2 Attacking prey versus searching for prey [98].

Hence, the optimal solution tends to diverge from the prey when, $\vec{A} > 1$ and converge towards the prey when $\vec{A} < 1$.

4.2.4 Hunting Mechanism

Grey wolves have the ability to recognize the location of prey and encircle them. The hunting is usually guided by α wolf. The β and δ wolves might also participate in hunting occasionally. In order to obtain the global optima more quickly, GWO improves the current best solution by using a weighting method. In GWO, the position update expression is weighted in every iteration as given in (4.7) and coefficient vectors are obtained using (4.5) and (4.6), where A_1, A_2 and A_3 are calculated using (4.3).

$$\begin{aligned} \overrightarrow{D}_\alpha &= \left|\vec{C}_1 \cdot \vec{X}_\alpha - \vec{X}\right| \\ \vec{D}_\beta &= \left|\vec{C}_2 \cdot \vec{X}_\beta - \vec{X}\right| \\ \vec{D}_\delta &= \left|\vec{C}_3 \cdot \vec{X}_\partial - \vec{X}\right| \end{aligned} \tag{4.5}$$

$$\begin{aligned} \vec{X}_1 &= \vec{X}_\alpha - \vec{A}_1 . \vec{D}_\alpha \\ \vec{X}_2 &= \vec{X}_\beta - \vec{A}_1 . \vec{D}_\beta \\ \vec{X}_3 &= \vec{X}_\delta - \vec{A}_1 . \vec{D}_\partial \end{aligned} \tag{4.6}$$

$$\vec{X}(j+1) = \frac{\vec{X}_1 + \vec{X}_2 + \vec{X}_3}{3} \tag{4.7}$$

4.3 Limitations of GWO

In case of conventional GWO, the location of the wolves within the entire community is updated by simple averaging of best locations. The GWO algorithm suffers from premature convergence and weak local searching ability. In order to take care this problem in the proposed work, a local search algorithm, called chaotic searching mechanism is combined with GWO to enhance the rate of convergence and avoid it from being stuck at local optima [112]. The evolved method is named as modified GWO

(MGWO) in this work. MGWO balances the exploration by modifying the position co-efficient to an exponentially decaying function. The convergence speed of the MGWO increases, when exploration is increased in comparison to exploitation. Moreover, this also avoids the local minima from being trapped. Weighted sum of best of the locations is taken instead of simple average of positions to achieve global optima.

4.4 Modified GWO Algorithm

The proper balance between exploration and exploitation guarantees accurate estimation of the global optima. Basic exploration and exploitation prevent the algorithm from finding global optima and also results into local optima stagnation. Generally, higher exploration of search space results in lower probability of local optima stagnation. Too much exploration is similar to too much randomness and will probably not give good optimization results. A right balance between these two exploration and exploitation can guarantee an accurate approximation of the global optimum. Thus, a balance between exploitation and exploration is a must. In MGWO, the transition between exploration and exploitation is generated by the adaptive values of a and A. In MGWO, half of the iterations are devoted to exploration ($|A| \geq 1$) and the other half are used for exploitation ($|A| < 1$). Exponential functions are used instead of linear function to decrease the value of a over the course of iterations. The function which gives the exponential decay for a during the iterations of MGWO is given as

$$a = 2\left(1 - \frac{m^2}{n^2}\right) \tag{4.8}$$

where m indicates the maximum number of iterations and n is the current iteration. The numbers of iterations used for exploration and exploitation are 60% and 40%, respectively.

GWO with chaotic search technique has been applied in this paper for the improvement of search efficiency and the reduction of the possibility of being trapped at the local optima [112]. The chaotic equation is defined as

$$x_{j+1} = \mu . x_j \left(1 - x_j\right) \tag{4.9}$$

where x_j is a variable ($j = 0,1,2 \cdots$) and μ is the control parameter. The procedure of chaotic local search is described as

$$cx_j^{n+1} = \mu . cx_j^n \left(1 - cx_j^n\right) \tag{4.10}$$

where cx_j^n represents the chaotic variable. *n* represents the iteration number.

The procedure of chaotic local search algorithm is as follows:

Step 1: Set *n* = 0 and map the decision variables x_j^n from the interval $(x_{min,\,j}, x_{max,\,j})$ to chaotic variables cx_j^n using

$$cx_j^n = \frac{x_j^n - x_{min,\,j}}{x_{max,\,j} - x_{min,\,j}} \tag{4.11}$$

Step 2: Determine the chaotic variables cx_j^{n+1} for the next iteration using (4.9).

Step 3: Convert the chaotic variables cx_i^{n+1} to decision variables x_j^{n+1} using

$$x_j^{n+1} = x_{min,\,j} + cx_j^{n+1}(x_{max,\,j} - x_{min,\,j}) \tag{4.12}$$

Step 4: The new solutions are evaluated with variables x_j^{n+1}.

Step 5: If the new solution achieves better performance or the maximum number of iterations is reached, take the new solution as chaotic local search; or else, modify *n* = *n*+ 1 and go back to Step 2.

4.4.1 Proposed Variable Weights in MGWO

In GWO, the searching and hunting process are governed by α wolf, whereas the β wolf plays less important role and the δ wolf plays lesser important role. During hunting process, α is nearest to the prey among three grey wolves; β and δ ranks second and third. So, the position of α wolf is mainly contributed in searching new individuals, while the importance of other wolves is ignored. This means that the weight of α should be near to 1 at the beginning, while the weights of the β and δ could be near zero. At the final state, the α, β and δ wolves should encircle the prey, which means that they have equal weights. So, the weight of the α is reduced and the weights of the β and δ arise in final stage of the algorithm. The previously described (4.7) is now modified in the proposed MGWO algorithm and given as

$$\vec{X}(j+1) = w_1.\vec{X}_1 + w_2.\vec{X}_2 + w_3.\vec{X}_3 \tag{4.13}$$

where w_1, w_2 and w_3 are the corresponding weights.

The weight of α, β and δ are denoted as w_1, w_2 and w_3. The weights should always satisfy $w_1 \geq w_2 \geq w_3$. Mathematically, the weight of α is changed from 1 to 1/3 during the searching procedure. At the same time, the weights of the β and δ is increased to 1/3 from 0.

The procedure for explaining the optimization problem using MGWO is as follows:

Step 1: Initialise MGWO parameters between upper and lower limits.

Step 2: Generate initial population randomly.

Step 3: Calculate fitness value of each grey wolf in the population and sort it according to fitness values.

Step 4: Select the first, second and third best fitness values as the positions of grey wolves α, β and ω respectively.

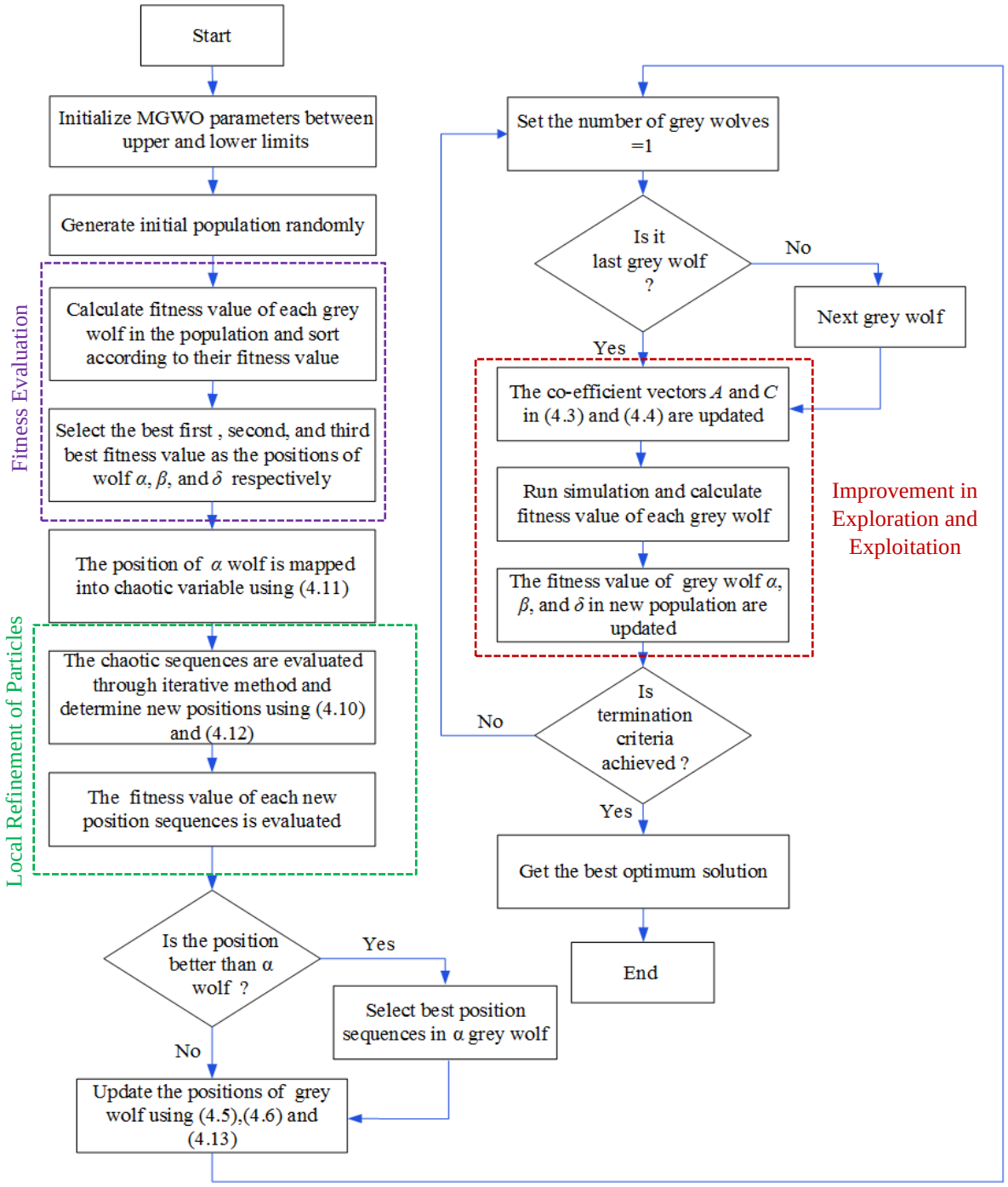

Fig. 4.3 Description of MGWO algorithm.

Step 5: The position of α wolf is mapped into chaotic variables using (4.11).

Step 6: The chaotic sequences are calculated through iterative technique and converted chaotic sequences are represented as new positions using (4.10) and (4.12).

Step 7: The fitness of new position sequences is evaluated.

Step 8: Update the positions of current grey wolves using (4.15) - (4.17).

Step 9: The co-efficient *A* and *C* in (4.5) and (4.6) and the parameter *a* in (4.13) are updated.

Step 10: The fitness values of grey wolves α, β and δ in new population are update till global optima is achieved.

Step 11: Repeat step 2 to 10, till the termination criteria is achieved.

The detailed flow chart of the optimization algorithm (MGWO) is shown in Fig. 4.3.

4.5 Implementation of SHE-PWM in MGWO Optimized HC-MLI

The proper objective function *f* is represented by the following mathematical equation

$$f = \min\left\{\left(100\frac{V_1^* - V_1}{V_1^*}\right)^4 + \sum_{s=2}^{S}\frac{1}{h_s}\left(50\frac{V_{h_s}}{V_1}\right)^2\right\} \tag{4.14}$$

subjected to

$$0 \le \theta_1 \le \theta_2 \ldots \theta_n < \frac{\pi}{2} \tag{4.15}$$

where h_s is the S_{th} harmonic order e.g., $h_2 = 5$, $h_3 = 7$, h_4=11 and h_5=15 and V_1^* represents the fundamental component of output voltage. The weighting factors $\left(\frac{1}{h_s}\right)$ defines the elimination in lower order harmonics. The number of iterations and population size in the algorithm are chosen as 200 and 100 respectively. The algorithm starts with the random initialization of wolves (switching angles) and the fitness of each wolf is then evaluated. In MGWO, chaotic iterative method is used for local refinement. Exponentially decaying position co-efficient stabilities exploration and exploitation mechanism. The algorithm is run for different modulation indices till the termination criteria is achieved. The plot of switching angles versus modulation index (m_a) is shown in Fig. 4.4. The graphs of fitness value versus modulation index for GA, PSO, GWO and MGWO are shown Fig. 4.5. The magnitude of lower order harmonics (5^{th}, 7^{th}, 11^{th} and 13^{th}) versus modulation index for the

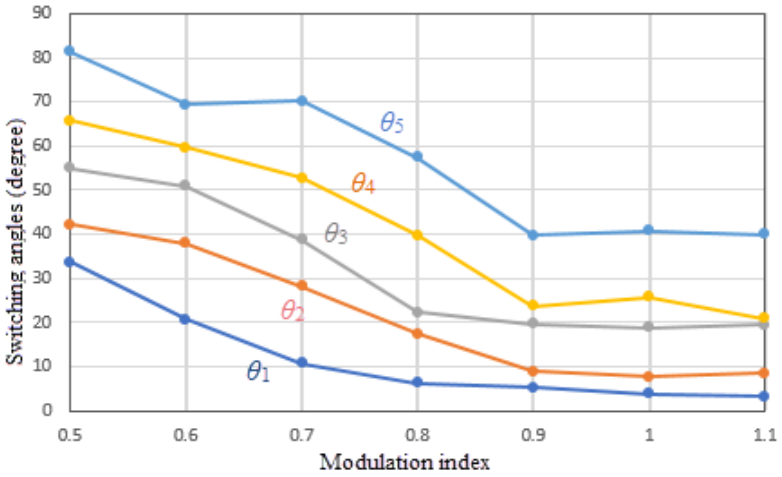

Fig. 4.4 Switching angles at different modulation index.

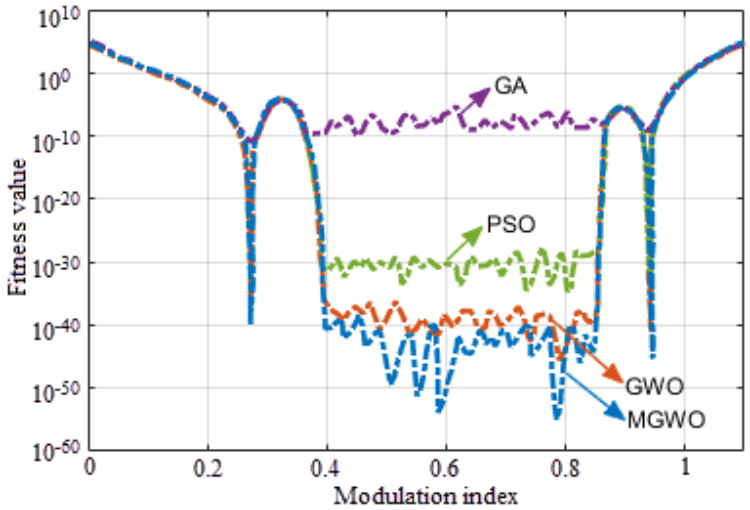

Fig. 4.5 Fitness value for MGWO, GWO, PSO and GA versus modulation index.

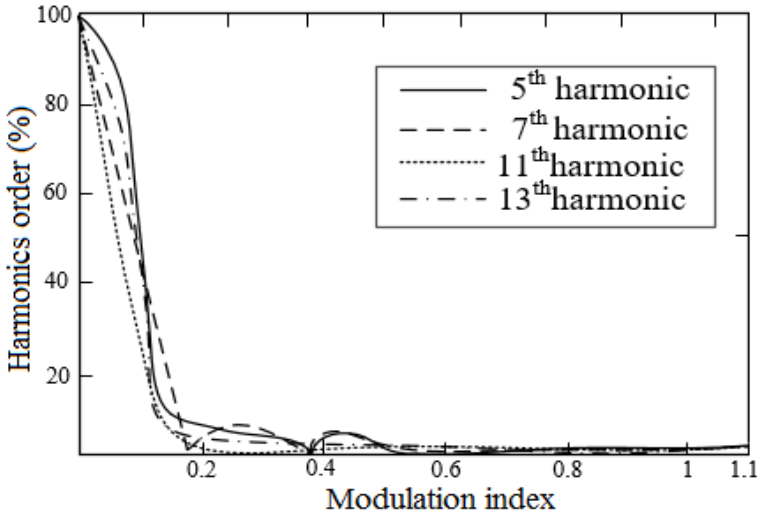

Fig. 4.6 The 5^{th},7^{th},11^{th} and 13^{th} harmonics versus modulation index.

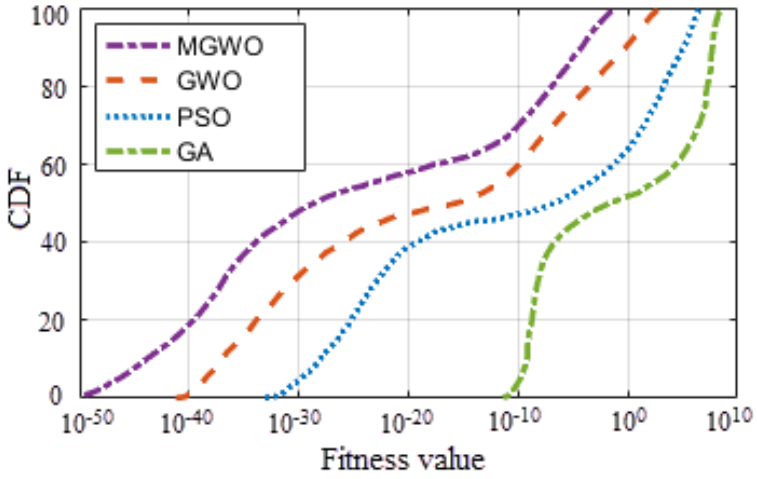

Fig. 4.7 Comparison of CDF versus fitness value for MGWO, GWO, PSO and GA.

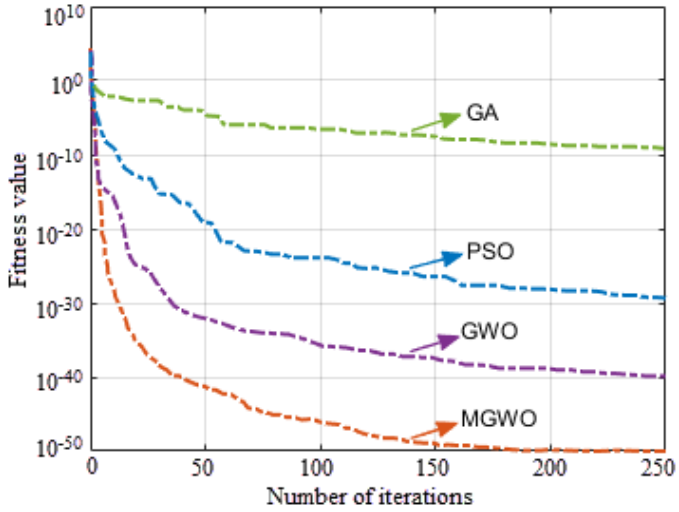

Fig. 4.8 Convergence plot of MGWO, GWO, PSO and GA versus number of iterations.

proposed MGWO are shown in Fig. 4.6. It can be observed from Fig. 4.6 that the lower order harmonics have decreased significantly. The cumulative distribution function (CDF) is evaluated to validate the usefulness of MGWO [114]. The comparison plots of CDF for GA, PSO and GWO with MGWO algorithm are shown in Fig. 4.7. The results obtained establish the superiority of MGWO in terms of rate of convergence as compared to GWO, PSO and GA. The convergence plots of fitness function versus number of iterations for MGWO, GWO, PSO and GA are shown in Fig. 4.8. It can be observed from Fig. 4.8 that the controller needs up to 200 iterations to obtain the optimal switching angle values in case of MGWO.

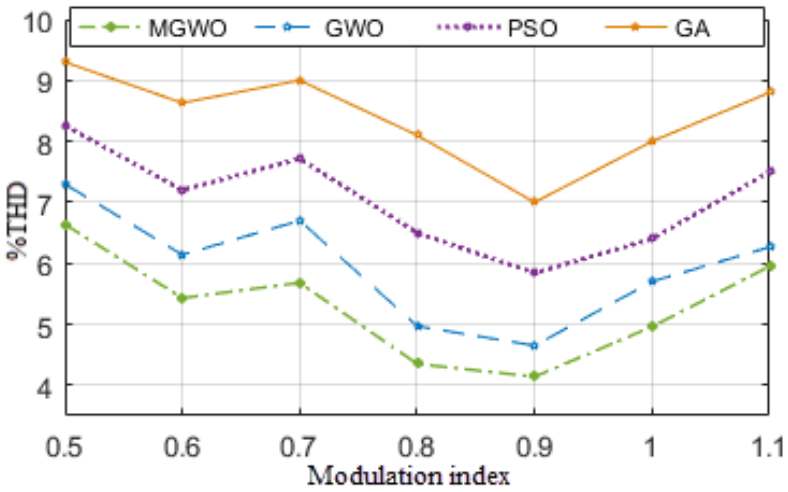

Fig. 4.9 Comparison of %THD for MGWO, GWO, PSO and GA at different modulation index.

Table 4.1
Parameters of MGWO, GWO, PSO and GA
No. of iteration=200 and Population size =100 at (m_a = 0.5)

Parameters	MGWO	GWO	PSO	GA
Fitness value	$6.7X10^{-46}$	$4.5X10^{-38}$	$5.3X10^{-30}$	$6.2X10^{-10}$
Convergence rate to global optima	very high	high	high	low

The %THD at different modulation indices for reported algorithms with proposed MGWO algorithm are shown in Fig. 4.9. The proposed MGWO optimized HC-MLI has better harmonic content than GA, PSO and GWO. The comparison of fitness values and convergence rate of different algorithms are given in Table 4.1. It can be concluded from Table 4.1 that the fitness value and convergence rate of MGWO is better than GA, PSO and GWO.

4.6 Simulation Verification

In order to verify the proposed work, a 1.5 kW three-phase, 11-level HC-MLI has been simulated in MATLAB/Simulink using proposed MGWO algorithm.

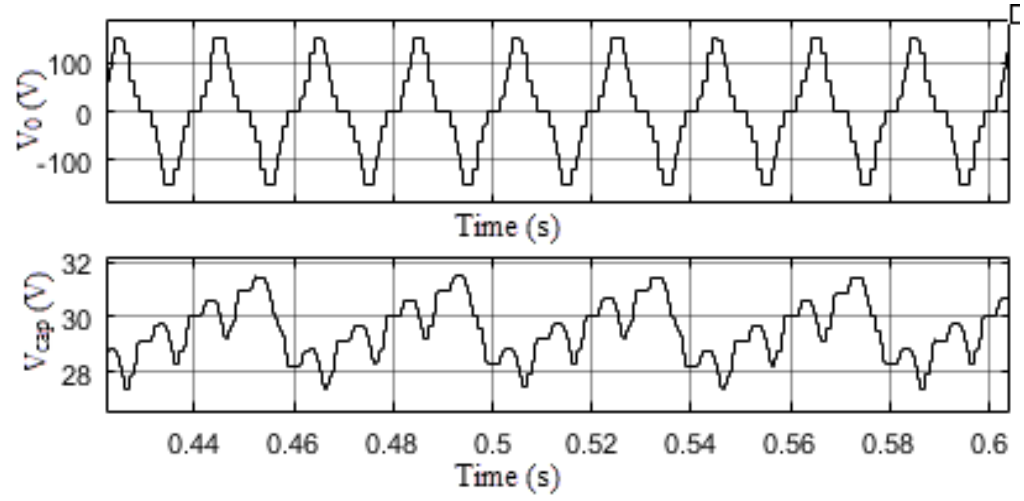

(a)

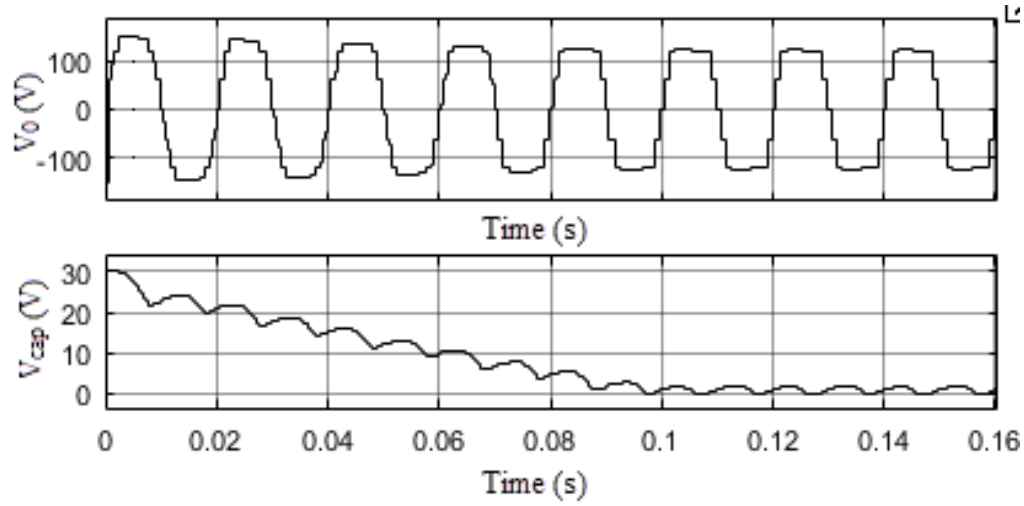

(b)

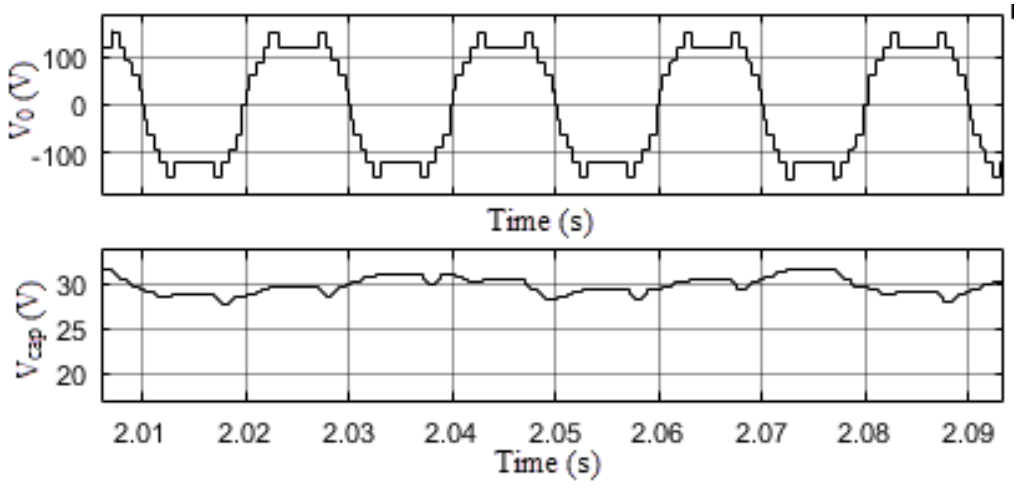

(c)

Fig. 4.10 Simulation results of MGWO optimized HC-MLI (Capacitor voltages). (a) V_0 and V_{cap} for modulation index (m_a) = 0.6. (b) V_0 and V_{cap} for m_a = 1.1 in case of unbalanced condition of capacitor. (c) V_0 and V_{cap} for m_a = 1.1 at balanced condition of capacitor voltage.

4.6.1 Operation at $m_a = 0.6$

From Fig. 4.4, the switching angles are obtained as $\theta_1 = 31.75$, $\theta_2 = 45.96$, $\theta_3 = 57.54$, $\theta_4 = 68.54$ and $\theta_5 = 85.34$. The waveform of V_0 and capacitor voltage V_{cap} of the HC-MLI are shown in Fig. 4.10(a). The average voltage across the capacitor is balanced at 30 V.

4.6.2 Operation at $m_a = 1.1$

Similarly, for $m_a = 1.1$, the switching angles are obatained as $\theta_1 = 5.33$, $\theta_2 = 8.57$, $\theta_3 = 20.56$, $\theta_4 = 25.39$ and $\theta_5 = 41.58$.

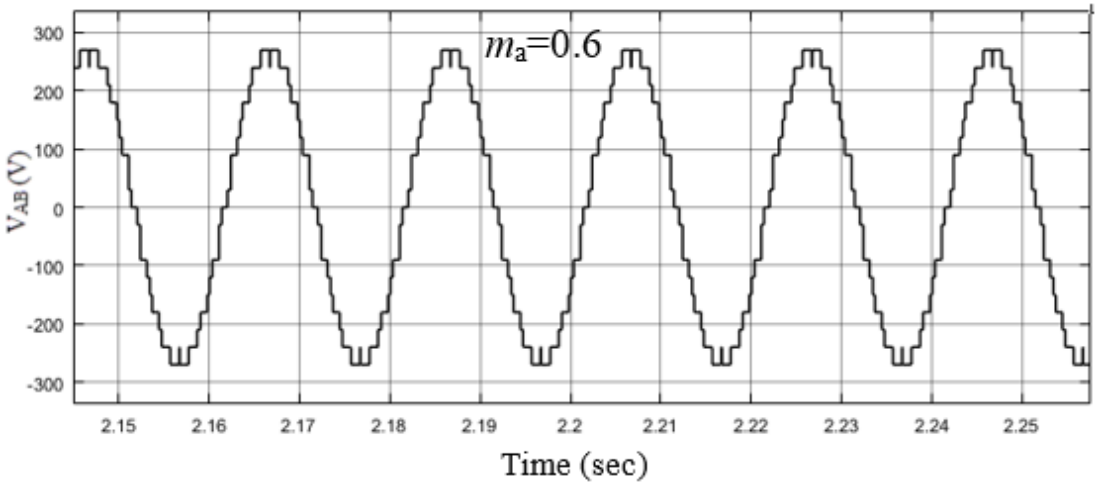

(a)

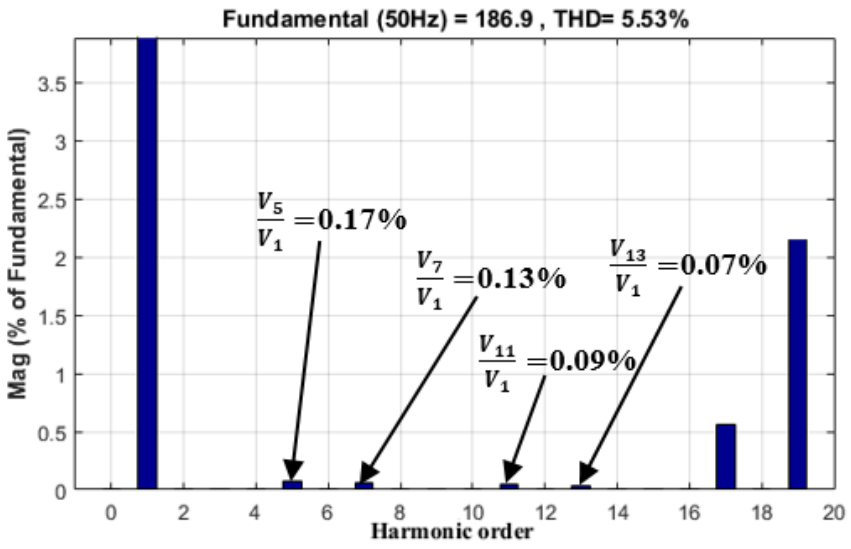

(b)

Fig. 4.11 Simulation results of MGWO optimized HC-MLI (Line voltages and harmonic spectrums).
(a) Line-line voltage (V_{AB}) for m_a 0.6. (b) Spectrum of harmonic analysis of V_{AB} for m_a 0.6.

With these switching angles, it is unable balance the capacitor voltage. Hence, in order to balance the capacitor, a third harmonic voltage is injected as discussed in 2.6.2 of chapter 2. Output voltage V_0 and capacitor voltage V_{cap} without and with capacitor balance are shown in Fig. 4.10(b) and (c) respectively. The average value of the capacitor voltage also gets balanced at 30 V for higher modulation index.

The output line voltage (V_{AB}) and its harmonic spectrum at $m_a = 0.6$ are shown in Fig. 4.11(a) and (b). It can be observed from Fig. 4.11(b) that lower order dominant harmonics (5^{th},7^{th}, 11^{th} and 13^{th}) have been eliminated from the output voltage of HC-MLI.

4.7 Experimental Validation

A 1.5 kW laboratory prototype is used to verify the performance of the proposed MGWO optimized three-phase, 11-level HC-MLI, as shown in Fig. 2.24 of chapter 2. The phase voltages (V_A, V_B and V_C) for resistive load at $m_a = 0.6$ are shown in Fig. 4.12(a) and are measured as 72.5 V. For *R-L* load, the output voltage V_A and output current I_L at $m_a = 0.6$ are shown in Fig. 4.12(b). The balancing of capacitor voltage at higher modulation index is also investigated experimentally. Fig. 4.12(c) shows the output phase *A* voltage (V_A) at $m_a = 1.1$ and three phase voltages (V_A, V_B and V_C) are shown in Fig. 4.12(d) and are measured as 111.5 V. The voltage of capacitor is balanced at 30 V. Hence, it confirms the balancing of capacitor voltage at higher m_a. The line-line voltage V_{AB} of the MGWO optimized HC-MLI at m_a=0.6 is shown in Fig. 4.13(a) and measured as 168.53 V. The harmonic spectrum analysis of V_{AB} for m_a=0.6 is shown in Fig. 4.13(b). From Fig. 4.13(b), it can be observed that the lower order harmonics such as 5^{th}, 7^{th}, 11^{th} and 13^{th} are reduced. Experimental results of line-line voltages (V_{AB}, V_{BC} and V_{CA}) at higher $m_a = 1.1$ are shown in Fig. 4.14. The output voltage V_{AC} and load current I_L after connecting filter inductor is shown in Fig. 4.15(a).

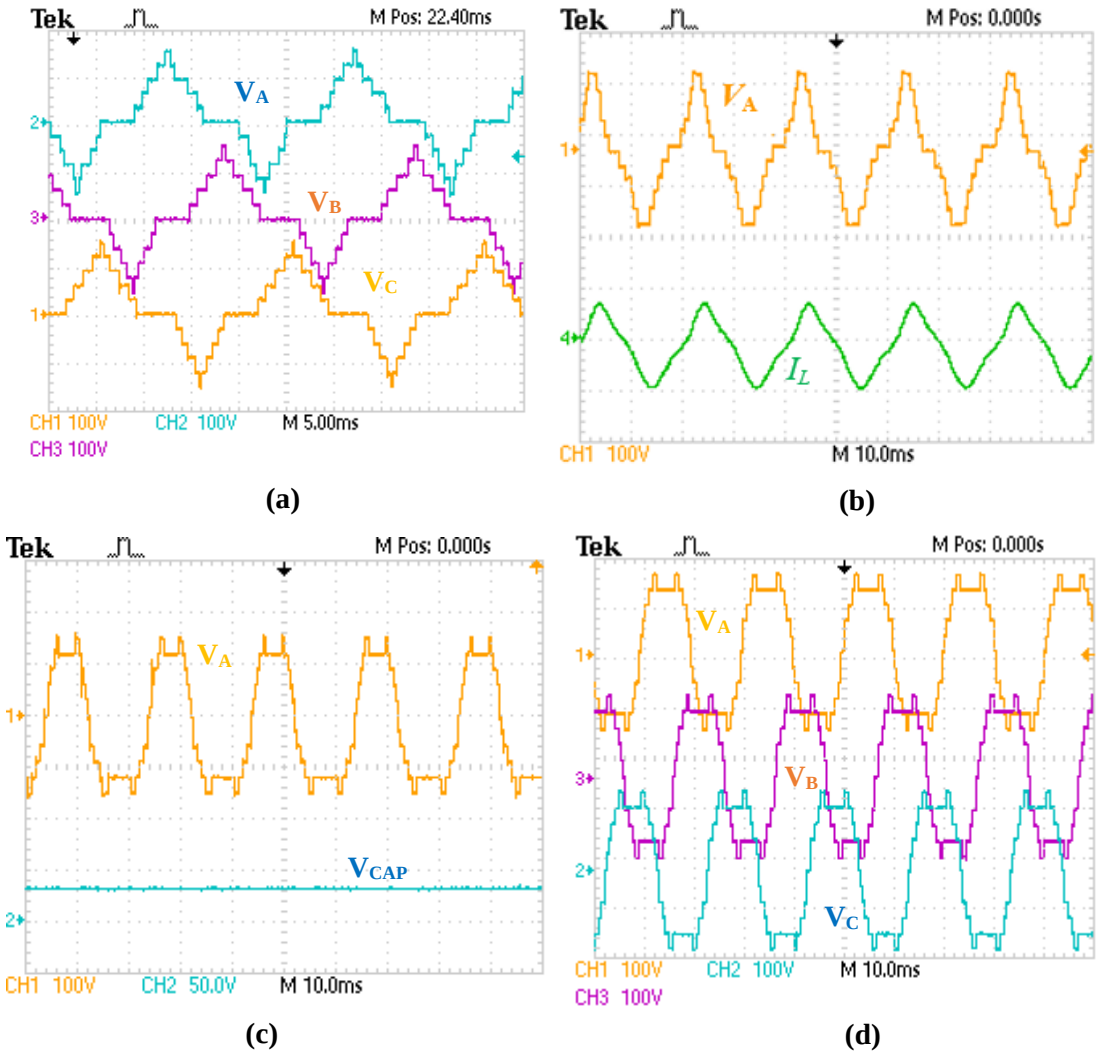

Fig. 4.12 Experimental results of MGWO optimized HC-MLI (Phase voltages).
(a) V_A, V_B and V_C for m_a 0.6. (b) V_A for inductive load for m_a 0.65. (c) V_A for m_a 1.1.(d) V_A, V_B and V_C for m_a 1.1.

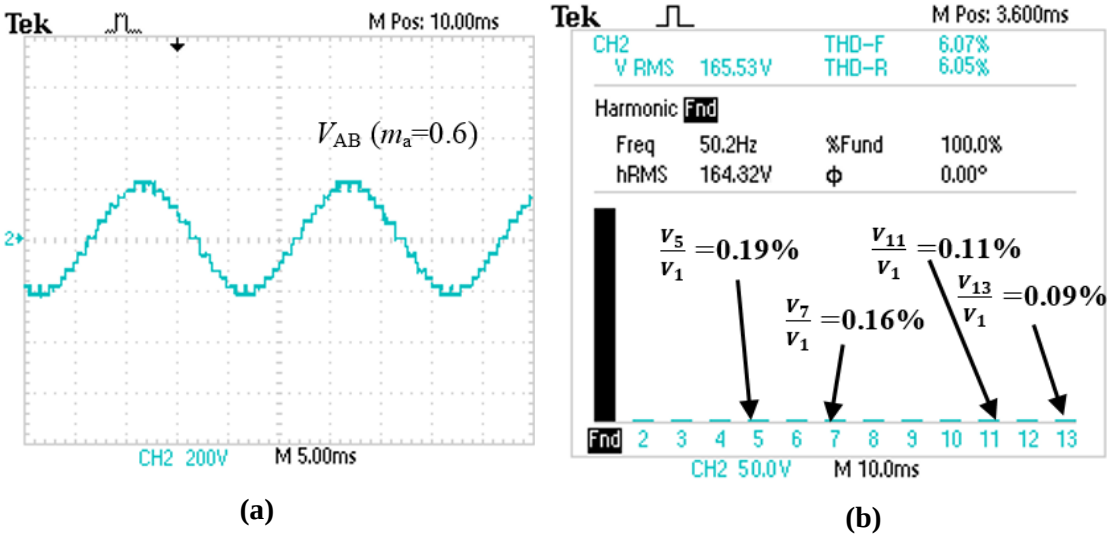

Fig. 4.13 Experimental result of line voltage at m_a 0.6.(a) Line -line voltage V_{AB} for m_a 0.6. (b) Spectrum of harmonic analysis of V_{AB} for m_a = 0.6.

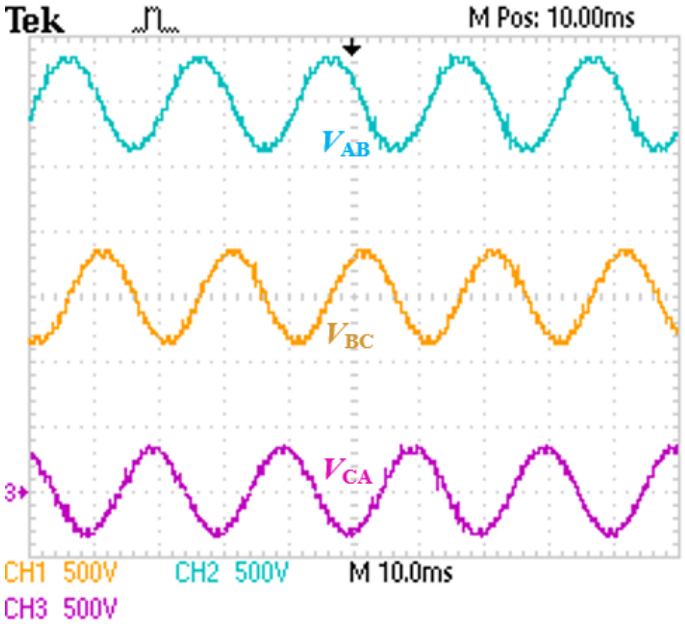

Fig. 4.14 Experimental results of MGWO optimized HC-MLI **(**Line-line voltage (V_{AB}) at m_a = 1.1).

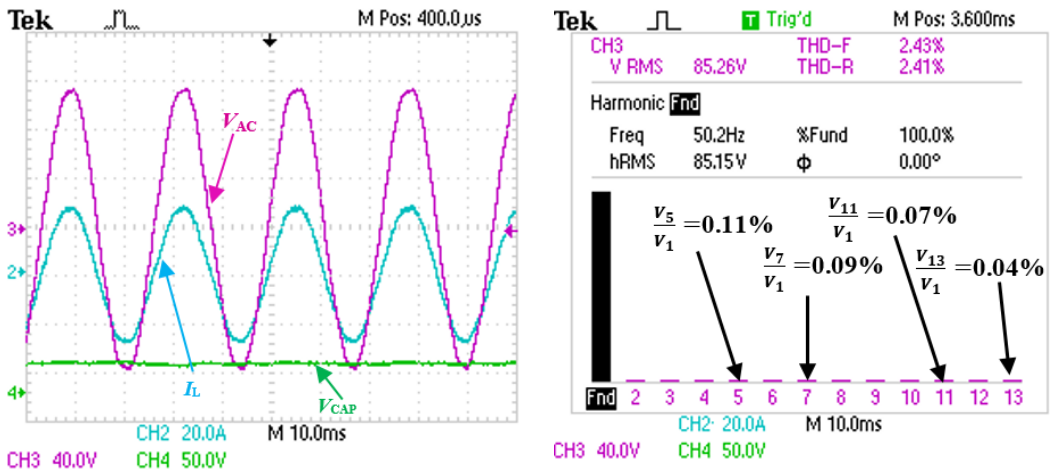

(a) **(b)**

Fig. 4.15 Experimental result of line voltage after connecting LC filter.
(a) Line-line voltage V_{AB} and voltage of capacitor V_{CAP} for m_a = 0.6. (b) Spectrum of harmonic analysis of V_{AB} for m_a = 0.6.

The output voltage of the HC-MLI is maintained at 85.2 V using closed loop control as discussed earlier for a load current of 16.8 A. The detailed harmonic analysis of V_{AC} at m_a = 0.6 after connecting LC filter is shown in Fig. 4.15(b) and harmonic magnitudes are within the IEEE Std 519-2014 [110].

Table 4.2
Comparison Between GWO [97] and MGWO

Modulation index (m_a)	**m_a = 0.6**					**m_a = 1.1**				
Harmonic order (h_s)	5^{th}	7^{th}	11^{th}	13^{th}	% THD	5^{th}	7^{th}	11^{th}	13^{th}	% THD
GWO [97]	0.2478	0.2235	0.1526	0.1229	6.13	0.3754	0.3158	0.2613	0.2145	6.24
MGWO	0.1963	0.1642	0.1103	0.0876	5.54	0.3268	0.2416	0.2127	0.1763	6.03

4.8 Comparison Between GWO and MGWO

A comparison between GWO [97] and MGWO is made as shown in Table 4.2, containing magnitude of lower order harmonics (5^{th}, 7^{th}, 11^{th} and 13^{th}) and %THD obtained through experimentation for GWO and MGWO algorithms at modulation indices m_a = 0.6 and 1.1, respectively. It can be observed that the lower order harmonics and %THD are further reduced in MGWO in comparison to GWO.

4.9 Comparison Among MPSO, MWO and MGWO

From the results obtained in chapters 2, 3 and 4, a comparison is made among MPSO, MWO and MGWO optimized HC-MLI using SHE-PWM for the same number of iterations and population size. It has been found that the running time of MPSO is more than MWO and MGWO. MPSO is more complicated than MWO and MGWO because it is a combination of a global exploration and local exploitation, which uses a complicated differential evolution mutation strategy. In the proposed MWO, the code complexity is less and it uses leadership hierarchy mechanism to obtain better refined solution as compared MPSO. The convergence rate of MWO is better than MPSO. The computational time required for digital implementation of MWO is also less than MPSO. The proposed MGWO gives improved results than MPSO and MWO; in terms of possibility of attaining global optima, higher rank of convergence, higher fitness value and harmonic content for the same population size and number of iterations.

Table 4.3
Comparison of % THD Among Proposed MPSO, MWO and MGWO

Modulation index	MPSO (%THD)	MWO (%THD)	MGWO (%THD)
0.5	8.41	8.23	7.52
0.6	7.53	7.09	6.41
0.7	7.69	6.78	6.12
0.8	5.23	5.01	4.33
0.9	4.78	4.50	4.14
1	5.03	4.67	4.55
1.1	5.64	5.11	4.01

Table 4.4
Performance comparison of MGWO, MWO and MPSO
No. of Iteration=200 and Population size =100 at (m_a=0.7)

Parameters	MGWO	MWO	MPSO
Convergence rate	Very high	Medium	Low
Computational time (sec)	1.116	1.132	1.953

The %THD comparison among MPSO, MWO and MGWO is given in Table 4.3. Table 4.4 gives the comparison of convergence rate and computational time for MGWO, MWO and MPSO. It can be observed from Tables 4.3 and 4.4 that the proposed MGWO gives better result in terms of harmonic content, convergence rate, and computational time.

4.10 Conclusion

In this chapter, MGWO optimized three-phase, 11-level HC-MLI is presented using SHE-PWM. The use of adaptive position co-efficient vector and exponentially decaying

function in MGWO gives improved results as compared to GWO. In MGWO, chaotic local search technique efficiently takes care of local optima, while weighted position control strategy enhances the convergence rate as compared to GA, PSO and GWO. MGWO also helps to obtain the global optima quickly as compared to GA, PSO and GWO and effectively eliminates lower order harmonics from the output voltage. Moreover, the proposed MGWO control strategy balances the capacitor voltage even at higher modulation indices by exploiting the redundancies of HC-MLI. The steady state and dynamic performance of the proposed MGWO optimized HC-MLI has been validated through simulation and experimentation. Further, a comparison among MPSO, MWO and MGWO has been carried out, which confirms the superiority of MGWO in terms of harmonic minimization and convergence rate.

It has been found that balancing of capacitor voltage is an inherent challenge in HC-MLIs. Several control schemes have been reported in the literature to achieve capacitor voltage balance in HC-MLIs, which makes the overall control complicated. The control schemes become even more complicated with the increase in number of output voltage levels of the HC-MLIs, as the increase in output voltage levels require more active and passive components along with increased number of DC voltage sources. Switched-capacitor multilevel inverters (SC-MLIs) have emerged in recent years as a promising MLI to counter these problems. SC-MLIs use lesser active and passive components along with reduced number of DC voltage sources as compared to HC-MLI. Also, the capacitor voltage is balanced inherently in SC-MLIs, without using extra control circuits and therefore the switching scheme is simple as compared to HC-MLI. The SC-MLIs given in literature are explored and two new topologies of them, namely diode assisted switched-capacitor MLI (DASC-MLI) and reduced voltage stress switched capacitor MLI (RVSC-MLI) are proposed using MGWO in the next two chapters.